Eurographics Conference on Visualization (EuroVis) 2017
B. Kozlíková, T. Schreck, and T. Wischgoll (Editors)

Short Paper

Interactive Level-of-Detail Visualization of 3D-Polarized Light Imaging Data Using Spherical Harmonics

C. Hänel[1,2] and A. C. Demiralp[1,2] and M. Axer[3] and D. Grässel[3] and B. Hentschel[1,2] and T. W. Kuhlen[1,2]

[1]Visual Computing Institute, RWTH Aachen University, Germany
[2]JARA-HPC, Aachen, Germany [3]Institute of Neuroscience and Medicine, Research Centre Jülich, Germany

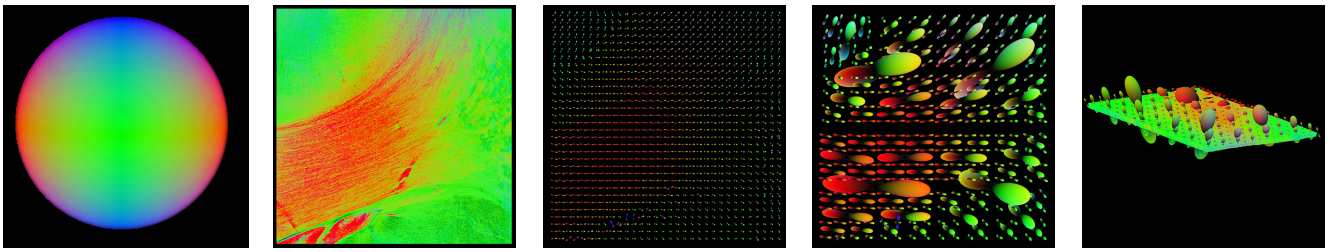

(a) **(b)** **(c)** **(d)** **(e)**

Figure 1: *Brain region in coronal direction from a vervet monkey (3072x3072x1 vectors). (a) Fiber orientation color code aligned to section. (b) Direct vector visualization. (c) Spherical harmonics representation at highest resolution (block size 48x48x1). (d) Combined visualization of multiple LODs. (e) Combined visualization of multiple LODs and vectors.*

Abstract

3D-Polarized Light Imaging (3D-PLI) provides data that enables an exploration of brain fibers at very high resolution. However, the visualization poses several challenges. Beside the huge data set sizes, users have to visually perceive the pure amount of information which might be, among other aspects, inhibited for inner structures because of occlusion by outer layers of the brain. We propose a clustering of fiber directions by means of spherical harmonics using a level-of-detail structure by which the user can interactively choose a clustering degree according to the zoom level or details required. Furthermore, the clustering method can be used for the automatic grouping of similar spherical harmonics automatically into one representative. An optional overlay with a direct vector visualization of the 3D-PLI data provides a better anatomical context.

CCS Concepts

•***Human-centered computing*** → ***Visualization techniques; Scientific visualization;***

1. Introduction

In the last decades, research on brain nerve fibers was mainly driven by diffusion-weighted Magnetic Resonance Imaging (dMRI) techniques such as Diffusion Tensor Imaging (DTI) or High Angular Resolution Diffusion Imaging (HARDI). In contrast, 3D-Polarized Light Imaging (3D-PLI) is a rather new, microscopic technique that allows for fiber exploration at much higher resolution in post-mortem brain tissue [AAG*11]. So far, there is no well-established visualization approach for 3D-PLI data. To this end, we propose a visualization by means of spherical harmonics at different levels of resolution that can be interactively chosen (see Figure 1).

The fundamental 3D-PLI data structure is a vector field indicating individual nerve fiber orientations. The similarity of PLI data to dMRI (though at a complementary resolution) is an appealing link between both techniques. Vilanova et al. [VZKL06] give an overview of visualization approaches for DTI data. Color coding the direction of a nerve fiber is a common technique (e.g., [JFM*04]). As each voxel is colored according to the direction of the underlying data this is a dense representation where a section view or the use of cutting planes is required to receive more information than a plain surface. Garyfallidis et al. [GBA*14] presented another approach that traces fiber bundles along their direction which results in a line representation that can be clustered in a further step to generate more structure within the data. Furthermore, interaction widgets allow for selective visualization of fiber bundles passing through a certain region of interest.

DOI: 10.2312/eurovisshort.20171145

Beyond DTI, which describes fiber distributions by means of a simple tensor, HARDI describes fiber distributions by means of orientation distribution functions (ODFs). ODFs integrate more detailed information per voxel than a single direction vector or a second-order tensor. Therefore, glyph-based representations of ODFs are an effective way for comprehensive visualization of high-resolution data. For example, Kindlmann [Kin04] presented superquadrics changing their shape based on eigenvalues and Hess et al. [HMH*06] employed spherical harmonics in order to represent an ODF of the fiber distribution in a single voxel. However, representing the data with one glyph per voxel eventually results in an incomprehensible visualization as it contains too much information that cannot be simultaneously perceived anymore due to visual clutter. As shown by Abbasloo et al. [AWHS16], this challenge can be met by employing different visualization techniques for an overview (volume rendered brain anatomy) down to a detailed view with glyphs.

The above-stated demands, such as dense information processing and visual clutter handling at low zoom levels, get even more significant for 3D-PLI data as the data resolution is much higher than for dMRI. Schubert et al. [SGP*16] provide different glyph types (e.g., lines, cuboids, cylinders) to visualize 3D orientation vector arrays while Axer et al. [ASG*16] employed spherical harmonics that integrate the information of the vector data. Both approaches use a color code representing the spatial direction. In comparison to Schubert et al., Axer et al. tackle visual clutter providing spherical harmonics at different levels of detail (LODs) by varying crop size and thereby the number of underlying vectors per ODF. The drawback of this approach is the lack of interactivity during adjustments. The spherical harmonics at different LODs are calculated on the original data, hence, the complete data set has to be reloaded to visualize a different level which inhibits the interactive visual analysis process of the exploration of fiber structures.

In this paper, we present an approach that enables the required interactive real-time modification of the resolution. It has been developed in close collaboration with neuroscience domain experts. In a pre-calculation step, the ODFs required for the spherical harmonics are calculated at full resolution. We then compute an octree enabling the fast visualization of different LOD representations. As the main limitation of our approach is the number of spherical harmonics that can be visualized simultaneously, we furthermore present an automatic, similarity-based clustering of the spherical harmonics that also supports to identify heterogeneous regions.

2. 3D-PLI Data

Before going into detail about deriving spherical harmonics and the visualization, this section provides an overview of the 3D-PLI technique and how the two data sets shown in the figures were created.

In 3D-PLI, the measured light intensities transmitted through the brain section sandwiched in between polarizing filters follow sinusoidal courses characterized by amplitude and phase depending on the spatial orientations of fiber axes contained in each voxel of tissue. These sinusoidal courses were used to derive two angles (ϕ_i and α_i) for each voxel i describing the fiber's axis in space with respect to the reference frame of the polarizers: the direction angle ϕ_i, which represents the azimuth of the projection of the principal fiber axis into the sectioning plane, and the inclination angle α_i, which is the angle of elevation between the principal fiber axis and the sectioning plane. Direction angle and inclination angle constitute the spherical coordinates of a unit vector, building a fiber orientation map (FOM) considering all voxels of the scanned brain section.

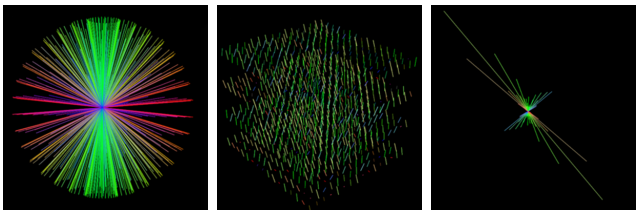

(a) (b) (c)

Figure 2: *(a) The unit hemisphere is binned into 32 longitudes times 16 latitudes = 512 bins, each of them represented by a bin vector. (b) Vector visualization of a 16x16x4 data block. (c) Radial histogram of this block.*

For the data used in this paper, 3D-PLI was applied to 60μm thick coronal sections through a formalin-fixed vervet monkey and a human brain, both acquired and prepared in accordance with the responsible animal research committee and ethics committee. Two polarimetric setups (providing pixel sizes of 1.3×1.3 μm^2 and 64×64 μm^2, resp.) were employed to carry out birefringence measurements and to give contrast to the orientation of individual nerve fibers and their tracts as described in [AGK*11].

3. Orientation Distribution Functions

ODFs describe the continuous spherical density of fiber orientations that can be approximated from the FOM. To this end, a radial histogram is created out of the FOM data (see Figure 2) which is then fitted to a spherical harmonics expansion.

In order to obtain a *radial histogram*, the FOM is divided into equally sized cubic blocks where the size is related to the actual size of the tissue represented by the vectors and not the number of vectors itself. Comparable to the approach by Axer et al. [ASG*16], the orientations within one block are quantized by mapping them on a defined number of bins of a unit hemisphere (see Figure 2a). The best match of a vector to a bin is identified by determining the maximum dot product between a 3D-PLI vector and a bin vector. The resulting radial histogram is a discrete estimation of the orientation probability density, i.e., the number of vectors in each bin related to its corresponding dihedral angle (see Figure 2c).

Spherical harmonics that form a set of orthonormal basis functions on the unit sphere (longitude $\theta = \frac{\pi}{2} - \alpha$, colatitude ϕ) can be approximated based on the radial histogram. A basis function $Y_l^m(\theta,\phi)$ with degree l and order m is defined as

$$Y_l^m(\theta,\phi) = \begin{cases} \sqrt{2}K_l^m cos(m\phi)P_l^m(cos(\theta)), & m > 0 \\ \sqrt{2}K_l^m sin(-m\phi)P_l^{-m}(cos(\theta)), & m < 0 \\ K_l^0 P_l^0(cos(\theta)), & m = 0 \end{cases} \quad (1)$$

with the associated Legendre polynomials P_l^m and the scaling factor

$$K_l^m = \sqrt{\frac{2l+1}{4\pi}\frac{(l-|m|)!}{(l+|m|)!}}. \quad (2)$$

As only an infinite number of basis functions $Y_l^m(\theta,\phi)$ and corresponding coefficients c_l^m would lead to an exact reconstruction of a spherical harmonic expansion, the spherical function f can be approximated by bounding the degree to $\bar{L}$ such that

$$\tilde{f}(\theta,\phi) = \sum_{l=0}^{\bar{L}} \sum_{m=-l}^{l} c_l^m \cdot Y_l^m(\theta,\phi). \quad (3)$$

The coefficients c_l^m of f are defined as

$$c_l^m = \int_0^{2\pi} \int_0^{\pi} f(\theta,\phi) Y_l^m(\theta,\phi) sin(\theta) d\phi d\theta. \quad (4)$$

With N being the number of bins in the radial histogram, c_l^m can be discretized to the Monte Carlo estimator for spherical functions

$$c_l^m \approx \frac{4\pi}{N} \sum_{n=0}^{N} f_n Y_l^m(\theta_n,\phi_n). \quad (5)$$

Furthermore, with the truncation to $\bar{L}$, Y_l^m can be expressed as rectangular matrix $\bar{Y}$ where the rows represent the bins and the columns the spherical harmonics coefficients up to $\bar{L}$. With the transposed matrix $\bar{Y}^T$ and h being a flattened 1D bin vector representation of the radial histogram that we aim to approximate the spherical harmonics expansion to, the coefficients can be rewritten in linear form

$$c \approx \frac{4\pi}{N} \bar{Y}^T h. \quad (6)$$

Based on this, we seek a set of coefficients c that best approximates the ODF. However, due to the discretization of the radial histogram and limiting the degree of the spherical harmonics to $\bar{L}$, an exact reconstruction is not possible such that Equation 3 can be seen as a linear least squares problem minimizing the 2-norm expression $||Yc-h||_2$. For reasons of numerical stability, we decided to apply a singular value decomposition. Thus, the final equation to be solved to receive the coefficients for the spherical harmonics is

$$c = V_{\bar{Y}} \Sigma_{\bar{Y}}^{-1} U_{\bar{Y}}^T h. \quad (7)$$

These coefficients describe the individual contribution of the spherical harmonics assembling the ODF. The entire set of ODFs of a data set are called an ODF map.

4. Visualization

3D-PLI is visualized in our approach based on two methods: direct vector field visualization and rendering of spherical harmonics based on the pre-calculation presented in Section 3. A direct vector visualization of the FOM is provided an as basic overview visualization modality (see Figure 1b) which color codes the vector direction in an RGB color scheme (red: left to right; green: anterior to posterior; blue: inferior to superior, see Figure 1a). On the one hand, it is hard to perceive individual orientations in the pile or—depending on the amount and observer distance—even the vectors itself (see Figure 1b). On the other hand, it is a fast visualization technique as only separate lines have to be rendered.

On top of that, we provide a second visualization method by means of spherical harmonics that integrates information of multiple vectors in order to avoid visual clutter for large amounts of data and emphasizes the fiber directions. The most natural way to visualize large vector arrays whose resolution exceeds screen resolution is their coarsening into cubic crops of arbitrary size and the integration of their directional distribution into a single glyph represented by the ODF. This has the benefit that directional information is preserved during visualization independent of the selected LOD. To approximate the coefficients of the spherical harmonics, first the angular location is determined by scaling the point for each spherical harmonic along the normal based on the corresponding ODF. Second, for constructing the spherical harmonic, points are sampled equally for $\theta \in [0,2\pi)$ and $\phi \in [0,\pi/2)$ on the unit hemisphere. Third, the sum of the spherical harmonics basis functions at each point (θ,ϕ) are weighted by the coefficients (see Equation 3). The sampling of the coefficients to obtain the points that define the spherical harmonic is realized in CUDA. These points are then used to create a triangle mesh for the actual visualization and for reasons of consistency, the applied color scheme is equal to the direct vector visualization. The spherical harmonics visualization can be interlaced or toggled with the direct vector visualization (see Figure 1) and 3D navigation is provided in an interactive manner.

4.1. Level-of-Detail Structure

With the approach presented above, we obtain a set of spherical harmonics coefficients as representations for a fixed cubic block size of vectors. As shown by Axer et al. [ASG*16], the size of the blocks can already be arbitrarily increased, which results in a less visual cluttered view onto the data as way less ODFs are presented. However, this has not yet been designed for an interactive change between these resolutions and the complete data set has to be reloaded each time another level is desired. Therefore, we introduce an interactive LOD approach that addresses this drawback and allows for visualization of multiple levels simultaneously (see Figure 1d).

When computing the ODFs for different block resolutions individually, the highest computational load stems from the singular value decomposition (Equation 7). Instead, the coefficients can be determined by component-wise summation of the coefficients of the higher LODs. Hence, we derive from Equation 3:

$$\tilde{f}(\theta,\phi) + \tilde{g}(\theta,\phi) = \sum_{l=0}^{\bar{L}} \sum_{m=-l}^{l} (f_l^m + g_l^m) \cdot Y_l^m(\theta,\phi). \quad (8)$$

Thus, the complete computation steps are only applied for the highest resolution of the data set and the spherical harmonics coefficients for each block are stored as leafs in an octree. The rest of the tree is constructed bottom-up by adding the coefficients of the child nodes to the parents node for each branch until the root is reached.

In comparison to Axer et al.'s work, our tree structure limits the block size to be always divided in half for each level. However, as the user can interactively select which LOD to visualize, this drawback is less relevant as the user can easily change to a higher resolution and compare the levels to determine if relevant information might get lost due to level switch.

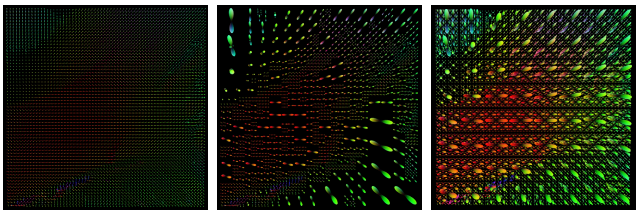

(a) (b) (c)

Figure 3: *(a) Spherical harmonics at highest resolution. (b) Automatic clustering of similar regions. (c) Comparing view with multiple overlayed LODs.*

4.2. Similarity Clustering

A further improvement of the presented approach is a local, automatic clustering of spherical harmonics (see Figure 3b). Visual clutter is reduced as redundant information is removed and the user is guided to more diverse regions with higher varieties in the fiber structure. Furthermore, this enables the visualization of larger regions of interest as the limitation of the graphics memory restricts the number of triangles that can be stored for each representative.

For the clustering, we employ the information in the octree. If all child nodes hold coefficients which are similar to the parent's coefficients, they are visualized by the parent's spherical harmonics representation and, thus, clustered. The similarity is specified by the L_2-difference between the parent and its children [KFR03]; the threshold that defines whether the difference is low enough to be considered for clustering is interactively defined by the user.

5. Results and Discussion

Our presented solution for visualizing 3D-PLI data through spherical harmonics is designed to work on consumer PCs as the data are processed block-wise. Hence, in comparison to Axer et al.'s approach [ASG*16], access to a supercomputer is not mandatory. However, as the implementation of the coefficient calculation and the visualization are realized in CUDA, the available GPU computing power and memory are limiting factors. Note that it is possible to store computed coefficients and, thus, hardware resources with better performance can be employed for preprocessing without requiring access during visual analysis of the resulting data.

For a radial histogram (90x50 bins) covering 180x180x1 FOM vectors, a block size of 4x4x1, and a maximum spherical harmonics degree of $\bar{L} = 12$, 2025 ODFs can be calculated in about 9.3 seconds on an NVIDIA GeForce 940M while for an NVIDIA GeForce 980 Ti the calculation is reduced to 2.7 seconds. Various parameters can be adjusted. For the pre-calculation these are: number of bins for the radial histogram, block size, and maximum degree for the spherical harmonics. For the visualization, sample resolution of the spherical harmonics and size of the displayed region can be interactively adjusted.

Furthermore, we facilitate an interactive change of the LOD to examine the data at different resolutions and guide the user's attention to regions with high variability by means of an optional, automatic clustering. Examining the data at very low LOD should be done cautiously. While the example of Figure 4a shows no obvious loss of information, in the second example (Figure 4b) the information of the fibers of the tapetum (part of the corpus callosum) are assimilated by surrounding spherical harmonics.

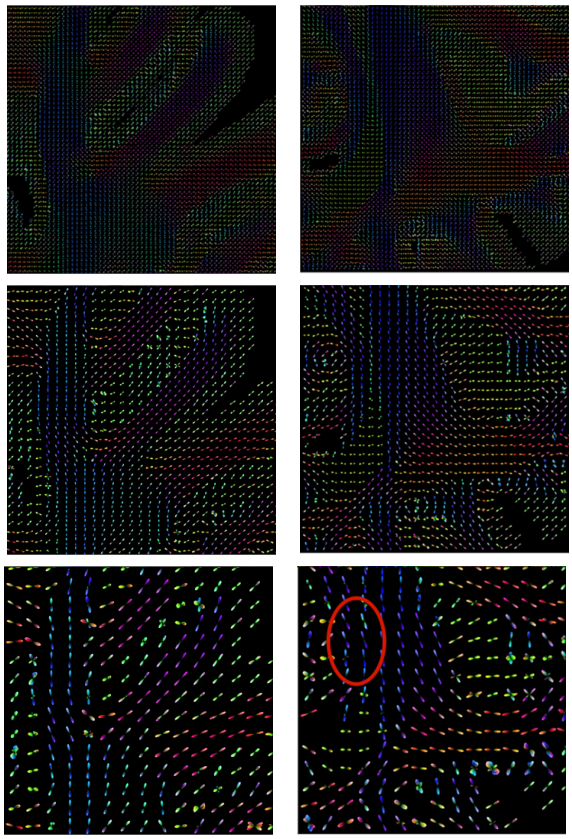

(a) (b)

Figure 4: *Relevance of LODs for regions in a human brain: (a) reduction in resolution shows no significant loss in information; (b) fiber information of the tapetum vanishes (red-circled area).*

Another benefit of real-time interaction is shown in Figure 1e. By rotating the data set, the user can better perceive the orientation of spherical harmonics. Thus, in comparison to a top view, spherical harmonics pointing out of slice are easily detectable.

6. Conclusion and Future Work

In this paper, we have presented an approach for visualizing 3D-PLI data. By means of spherical harmonics, multiple voxels are combined into one representation to reduce visual clutter. Interactive adjustment of the presented LOD allows for faster analysis of the data as it was possible before. Furthermore, we see great potential in applying this clustering techniques also to dMRI modalities.

For future work, we plan to enhance our prototype by linking the fiber to an anatomy visualization to provide better spatial context. Furthermore, we want to optimize the approximation by spherical harmonics also for a supercomputer to speed up the integration of new data sets. This should comprise a fast transfer of interactively selected regions onto a local machine for visualization purposes.

Acknowledgments

The research leading to these results has received funding from the European Union's Horizon 2020 research and innovation programme under grant agreement No 720270 (HBP SGA1) and from the Helmholtz Portfolio Theme "Supercomputing and Modeling for the Human Brain".

References

[AAG*11] AXER M., AMUNTS K., GRÄSSEL D., PALM C., DAMMERS J., AXER H., PIETRZYK U., ZILLES K.: A novel approach to the human connectome: Ultra-high resolution mapping of fiber tracts in the brain. *NeuroImage 54*, 2 (2011), 1091–1101. 1

[AGK*11] AXER M., GRASSEL D., KLEINER M., DAMMERS J., DICKSCHEID T., RECKFORT J., HUTZ T., EIBEN B., PIETRZYK U., ZILLES K., AMUNTS K.: High-resolution fiber tract reconstruction in the human brain by means of three-dimensional polarized light imaging. *Frontiers in Neuroinformatics 5* (2011), 34. 2

[ASG*16] AXER M., STROHMER S., GRÄSSEL D., BÜCKER O., DOHMEN M., RECKFORT J., ZILLES K., AMUNTS K.: Estimating fiber orientation distribution functions in 3D-Polarized Light Imaging. *Frontiers in Neuroanatomy 10*, 40 (2016). 2, 3, 4

[AWHS16] ABBASLOO A., WIENS V., HERMANN M., SCHULTZ T.: Visualizing Tensor Normal Distributions at Multiple Levels of Detail. *IEEE Transactions on Visualization and Computer Graphics 22*, 1 (2016), 975–984. 2

[GBA*14] GARYFALLIDIS E., BRETT M., AMIRBEKIAN B., ROKEM A., VAN DER WALT S., DESCOTEAUX M., NIMMO-SMITH I.: Dipy, a library for the analysis of diffusion MRI data. *Frontiers in Neuroinformatics 8* (2014), 8. 1

[HMH*06] HESS C. P., MUKHERJEE P., HAN E. T., XU D., VIGNERON D. B.: Q-ball reconstruction of multimodal fiber orientations using the spherical harmonic basis. *Magnetic Resonance in Medicine 56*, 1 (2006), 104–117. 2

[JFM*04] JELLISON B. J., FIELD A. S., MEDOW J., LAZAR M., SALAMAT M. S., ALEXANDER A. L.: Diffusion tensor imaging of cerebral white matter: a pictorial review of physics, fiber tract anatomy, and tumor imaging patterns. *American Journal of Neuroradiology 25*, 3 (2004), 356–369. 1

[KFR03] KAZHDAN M., FUNKHOUSER T., RUSINKIEWICZ S.: Rotation Invariant Spherical Harmonic Representation of 3D Shape Descriptors. In *Proceedings of the 2003 Eurographics/ACM SIGGRAPH Symposium on Geometry Processing* (Aire-la-Ville, Switzerland, Switzerland, 2003), SGP '03, Eurographics Association, pp. 156–164. 4

[Kin04] KINDLMANN G.: Superquadric Tensor Glyphs. In *Proceedings of the Sixth Joint Eurographics-IEEE TCVG Conference on Visualization* (2004), Eurographics Association, pp. 147–154. 2

[SGP*16] SCHUBERT N., GRÄSSEL D., PIETRZYK U., AMUNTS K., AXER M.: Visualization of Vector Fields Derived from 3D Polarized Light Imaging. In *Bildverarbeitung für die Medizin 2016*. Springer, 2016, pp. 176–181. 2

[VZKL06] VILANOVA A., ZHANG S., KINDLMANN G., LAIDLAW D.: An Introduction to Visualization of Diffusion Tensor Imaging and its Applications. In *Visualization and Processing of Tensor Fields*. Springer, 2006, pp. 121–153. 1